IEEE Access
Multidisciplinary : Rapid Review : Open Access Journal

Received November 16, 2021, accepted November 28, 2021, date of publication November 30, 2021, date of current version December 10, 2021.

Digital Object Identifier 10.1109/ACCESS.2021.3131652

MIMO Radar Waveform Joint Optimization in Spatial-Spectral Domain for Anti-Interference

CHUN-HUA CHU[1,2], QUN ZHANG[1], AND YI-JUN CHEN[1,3]

[1]Information and Navigation College, Air Force Engineering University, Xi'an, Shaanxi 710077, China
[2]Mechanical and Electrical Engineering College, Hainan University, Haikou, Hainan 570228, China
[3]College of Information Engineering, Engineering University of PAP, Xi'an, Shaanxi 710078, China

Corresponding author: Qun Zhang (afeuzq@163.com)

This work was supported in part by the National Natural Science Foundation of China under Grant 61801516, and in part by the Hainan Provincial Natural Science Foundation of China under Grant 621QN0872.

ABSTRACT Aiming at the target detection problem of MIMO radar under the condition of both spatial and spectral domain interferences, a waveform design method for MIMO radar based on joint optimization of spatial and spectral domain interferences suppression in multi-target scenarios is proposed. Compared with the traditional synthetic waveform method based on the transmitting signal covariance matrix, this method directly performs waveform design in the space-spectral domain in turn, considering target characteristics and spatial-spectral environment comprehensively. Firstly, according to the target characteristics and energy allocation strategy, the fast time transmission pulse set is divided into a group of sub-pulse sets whose number equals to the number of targets. Meanwhile a set of transmit filter weighting factor vectors are introduced and the number of vectors equals to the number of spatial interferences. Furthermore, the spatial waveform optimization model is constructed according to the pattern matching criterion, subjecting to the peak-to-average power ratio of the transmitted signal. The sub-pulse sets are obtained through convex optimization, and the full matrix of the emission waveform is formed by the sub-pulse sets. Then, according to the invariability of radar transmit pattern with changing the initial phase of the sub-pulse, the transmitted waveform with desired beam pattern and spectrum distribution is obtained by optimizing the initial phase matrix through convex optimization. Finally, the optimized transmit waveform of MIMO radar with the ability of simultaneously suppressing space frequency interferences is generated. The simulation results prove the effectiveness of the proposed method.

INDEX TERMS MIMO radar, beam pattern matching, spatial-spectral domain anti-jamming, waveform synthesis.

I. INTRODUCTION

Multiple input multiple output (MIMO) radar is regarded as an emerging radar system, which has more freedoms than traditional phased-array radar by probing independent signals via different antennas and waveform diversity at the receiving end. According to the characteristics of antenna layout and signal processing, MIMO radar can be divided into distributed MIMO and centralized MIMO. Distributed MIMO radar can make full use of the scattering characteristics of the target at different angles to improve the spatial resolution of the radar [1], while centralized MIMO radar uses waveform diversity to form a larger virtual array aperture which improves the performance of radar parameter estimation, target recognition and interference suppression, such as interference cancellation in multi-beam schemes [2].

Traditional centralized MIMO radar usually emits orthogonal waveforms from different antennas to form an omnidirectional beam pattern [3]. At the receiving end, a larger virtual array aperture is obtained through waveform matching, and then the transmission waveform diversity gain is obtained. However, when the distribution map of targets is relatively concentrated or spatial location can be roughly known, the wide beam not only causes the space waste of the transmission power, but also makes the corresponding virtual array element equivalent received signal strength weak, which is not conducive to the detection and recognition of the target, especially weak target.

Aim to this issue, the correlation of the transmitted waveforms among different elements can be applied to design

The associate editor coordinating the review of this manuscript and approving it for publication was Brian Ng.

a MIMO radar beam pattern with some shape to make the emission energy focusing in a specific spatial range [4]–[7]. In order to avoid directly optimizing the covariance matrix and designing the waveform matching the desired pattern, S. Ahmed established an unconstrained optimization model of the base waveform weighting matrix, used the classic Newton gradient method to solve the weighting matrix, and then obtained the desired beam pattern and emission waveform, but the resulting peak-to-average-power ratio (PAPR) of the synthesized waveforms were greater than 1 [4]. N. Pandey proposed two algorithms of synthesizing beam pattern by optimizing transmitted signal covariance matrix, but didn't consider the transmit waveform synthesis [5]. Xu constructed an optimization model of the emission waveforms based on the principle of minimizing integrated sidelobes under the premise of beam pattern matching, and the emission waveform can be synthesized according to the optimized weight matrix and limited number independent orthogonal baseband waveforms [6]. Ni proposed a decoupled directional range indication scheme based on coprime FDA, which can produce a beampattern with a more focused energy distribution and lower sidelobes, but without additional hardware complexity requirements [7].

All of the above methods can form desired beam pattern, and synthesizes emission waveforms except [5]. The classical waveform synthesis algorithm according to the covariance matrix is cyclic iterations algorithm (CA) [8]. In addition to the above-mentioned documents, there are also many researches on waveform optimization methods based on various prior information, practical constraints and beam pattern matching criteria [9], [10]. Fan presented two new design methods to achieve the minimum peak sidelobe transmit beampattern under the constant modulus constraints. The proposed algorithms have an advantage over several existing methods in terms of low PSL, ripple control and deep null [9]. Cheng presented a joint design method of MIMO radar waveform transceiver with PAPR and similarity constraint (SC) [10]. Both [9] and [10] solved nonconvex optimization problem and had the superiority over existing methods. The prior information of target and interference can be obtained through multiple methods [11]–[14].

Although many algorithms and discussions have been proposed on the MIMO radar waveform design, either in spatial domain [15], [16] or in spectral domain [17]–[19], or joint in spatial-temporal domains [20]–[22], few attentions have been paid in both spatial domain and spectral domain. In fact, MIMO radar is dually affected by spatial interference and spectral interference in practical applications. Wang conducted similar research on single target and single spectral interference scenes via the sequential optimization (SO) in spatial and spectral domains [23]. P.-M. McCormick introduced a joint spectrum/beampattern design method of MIMO radar emission based on alternating projections [24]. The method focuses on the power design within the bandwidth.

Considering the complexity of multi-domain joint optimization and computational complexity, most of the above-mentioned methods cannot meet the requirements of real-time signal processing. This paper aims to address multi-domain joint optimization with a fast algorithm, designing MIMO radar waveform based on prior information to suppress interferences from both spatial domain and spectral domain in a multi-target scenario. In order to achieve this goal, the optimization process can be carried out in two stages. Firstly, transmission pulse set is divided into subsets of which the number equals to the number of targets, according to the energy allocation strategy, and a weighting matrix is introduced. Meanwhile, the optimization model which can suppress the spatial interference is formed based on the beam matching criterion. The solution of sub-pulse sets can be found in polynomial-time via convex optimization. Secondly, based on the fact that changing the initial phase of each sub-pulse will not influence the shape of spatial beam pattern, a phase changing auxiliary vector is introduced to build a quadratic modal subjecting to a constant modulus constraint, which is nonconvex. By relaxing non-convex constraint and adding a PAPR constraint, the original problem becomes a convex programming problem, and the solution after optimization satisfies the spatial-spectral domain requirements. Finally, the global optimal waveforms are achieved via the sequential optimizations in spatial and spectral domains and numerical comparisons are conducted to evaluate the proposed design approach.

The rest of the paper is organized as follows. The signal model and optimization ideas are presented in Section II. In Section III, both the spatial optimization model and spectral optimization model are developed and discussed, finally the solution is obtained. Section IV presents various numerical simulations and conclusions are finally drawn in Section V.

Notation: We use $(\cdot)^T$ to denote the transpose, $()^*$ for the conjugate, and $(\cdot)^H$ for the conjugate transpose. Hadamard product operation is denoted as $\odot$, and Kronecker product is denoted as $\otimes$ or *kron*(). We use $vec(\cdot)$ for the change from matrix to vector by column.

II. SIGNAL MODEL AND PROBLEM DESCRIPTION

Consider a centralized MIMO radar system equips with M antennas and the transmit array is a uniform linear array (ULA) with half-a-wavelength element separation. The total transmit power of radar system is $E = M$. Without loss of generality, the transmit signal matrix is denoted as

$$S = [\boldsymbol{s}(1), \boldsymbol{s}(2), \ldots, \boldsymbol{s}(N)] = [s_1\ s_2\ \ldots\ s_M]^T \in C^{M\times N}$$
$$s_m = [s_m(1)\ \ldots\ s_m(n)\ \ldots\ s_m(N)], \quad 1 < m < M,\ 1 < n < N \tag{1}$$

where N is the code length, number of samples within a coherent processing interval; $\boldsymbol{s}_m$ stands for the signal sequence emitted by the mth array element; $\boldsymbol{s}(n)$ denotes nth sampled transmit sequence.

As the spatial location of the target and the interference is predictable or known as prior information, our method is divided into two steps. In spatial domain, emission sub-pulse sets and anti-jamming weighting factor vectors are designed through convex optimization, under the beam pattern matching criteria and subjecting to PAPR constraint. Then according to the invariability of radar transmit pattern with changing the initial phase of each sub-pulse, the transmitted waveform with desired beam pattern and spectrum distribution is obtained through optimizing the initial phase changing vector by means of convex optimization after relaxation of nonconvex constraint.

A brief discussion is made to prove the rationality of the optimization sequence.

Assume the modulus of signal is γ, then the emission signal of the pth element and the qth element can be expressed as

$$\begin{aligned} s_p &= \gamma \left[e^{j\theta_{p1}} \quad e^{j\theta_{p2}} \quad \ldots \quad e^{j\theta_{pN}} \right] \\ s_q &= \gamma \left[e^{j\theta_{q1}} \quad e^{j\theta_{q2}} \quad \ldots \quad e^{j\theta_{qN}} \right], \quad p \neq q. \end{aligned} \tag{2}$$

The covariance matrix formed by these two sequences is

$$\begin{aligned} \boldsymbol{R}_{pq} &= \begin{bmatrix} s_p s_p^H & s_p s_q^H \\ s_q s_p^H & s_{m_2} s_q^H \end{bmatrix} \\ &= \begin{bmatrix} N\gamma^2 & \gamma^2 \sum\limits_{n=1}^{N} e^{j(\theta_{pn}-\theta_{qn})} \\ \gamma^2 \sum\limits_{n=1}^{N} e^{j(\theta_{qn}-\theta_{pn})} & N\gamma^2 \end{bmatrix} \end{aligned} \tag{3}$$

The beam pattern formed by the emission signals of the two elements in the θ direction can be expressed as

$$P_{pq}(\theta) = \boldsymbol{a}_{pq}^H(\theta)\boldsymbol{R}_{pq}\boldsymbol{a}_{pq}(\theta) \tag{4}$$

where $\boldsymbol{a_2}(\theta) = [e^{-j(p-1)\pi \sin\theta} \ e^{-j(q-1)\pi \sin\theta}]^T$ is the steering vector of the two elements in the θ direction.

The energy distribution of the emission sequence at frequency f can be expressed as

$$\begin{aligned} S_p(f) &= \left| \sum_{n=1}^{N} s_p(n) e^{-j2\pi f(n-1)} \right|^2 = \gamma^2 \left| \sum_{n=1}^{N} e^{j\theta_{pn}} e^{-j2\pi f(n-1)} \right|^2 \\ S_q(f) &= \left| \sum_{n=1}^{N} s_q(n) e^{-j2\pi f(n-1)} \right|^2 = \gamma^2 \left| \sum_{n=1}^{N} e^{j\theta_{qn}} e^{-j2\pi f(n-1)} \right|^2 \end{aligned} \tag{5}$$

When changing the phase θ_{in}, $i = p, q$ of the nth $(n = 1 \ldots N)$ code of the emission waveform, the covariance matrix $\boldsymbol{R}_{pq}$ and the beam pattern $P_{pq}(\theta)$ will not be changed, but $S_p(f)$ and $S_q(f)$ will be changed.

It indicates that the spatial domain and the spectral domain optimization can be completed successively. First, a desired beam pattern is formed through the spatial optimization, and then the spectral design of the emission waveform is performed without changing the beam pattern.

III. WAVEFORM DESIGN BASED ON JOINT OPTIMIZATION IN SPATIAL AND SPECTRAL DOMAINS

A. WAVEFORM DESIGN BASED ON BEAM PATTERN MATCHING

The far-field received signal of the n th sample in the direction θ is

$$s(n, \theta) = \boldsymbol{a}^H(\theta)\boldsymbol{s}(n) \tag{6}$$

where $\boldsymbol{a}(\theta) = [1, e^{-j\pi \sin(\theta)}, \ldots, e^{-j(M-1)\pi \sin(\theta)}]^T$ is the steering vector of the array at the θ direction. The average energy distribution of the radar transmitted signal in space can be expressed as

$$P(\theta) = \frac{1}{N}\sum_{n=1}^{N} \boldsymbol{a}^H(\theta)\boldsymbol{s}(n)\boldsymbol{s}^H(n)\boldsymbol{a}(\theta) = \boldsymbol{a}^H(\theta)\boldsymbol{R}\boldsymbol{a}(\theta) \tag{7}$$

where $\boldsymbol{R} = \frac{1}{N}\sum\limits_{n=1}^{N} \boldsymbol{s}(n)\boldsymbol{s}^H(n) = \frac{1}{N}\boldsymbol{S}\boldsymbol{S}^H$ is the theoretical covariance matrix of radar emission waveform. Most of the existing waveform design method for beam pattern matching is generally to obtain the transmit waveform correlation matrix $\boldsymbol{R}$ first, and then to synthesize waveform according to $\boldsymbol{R}$ by optimization constrained non-convex quadratic model. The proposed method is completely different.

Assume that the number of the spatial targets is K and the number of the measurable interference is J, which are obtained according the prior information. The targets and interference are located in spatial direction set Θ_K and Φ_J respectively. θ_k and ϕ_j denote respectively the angle of the kth target and the jth interference. Here, $\theta_k \in \Theta_K, k = 1, \ldots, K$, $\phi_j \in \Phi_J, j = 1 \ldots J$,and $\Theta_K \cap \Phi_J = \{\}$. According to the energy allocation strategy, the transmit waveform matrix is divided as follows

$$\begin{aligned} \boldsymbol{S} &= [s(1), s(2), \ldots, s(N)] = \left[\boldsymbol{s}_1^\dagger | \ldots |\boldsymbol{s}_{\boldsymbol{k}}^\dagger | \ldots |\boldsymbol{s}_K^\dagger\right] \\ &= \boldsymbol{S}^\dagger \in C^{M\times N}, \quad K \ll N \\ \boldsymbol{s}_{\boldsymbol{k}}^\dagger &= [s_k^\dagger(1), s_k^\dagger(2), \ldots, s_k^\dagger(N_k)], \quad \sum_{k=1,2,\ldots,K} N_k = N, \\ & k = 1, 2, \ldots, K, \quad \sum_{k=1,2,\ldots,K} E_k = E \end{aligned} \tag{8}$$

where $\boldsymbol{s}_{\boldsymbol{k}}^\dagger \in C^{M\times N_k}$ denotes the sub-pulse set pointing to the kth target, consisting of N_k sub-pulses. The scale of N_k sub-pulse sets is determined by the energy distribution strategy according to the prior information. E_k is the emission power of $\boldsymbol{s}_{\boldsymbol{k}}^\dagger$ and θ_k is the main energy radiation direction of $\boldsymbol{s}_{\boldsymbol{k}}^\dagger$. The steering vector of the kth target direction and the jth interference direction can be denoted as $\boldsymbol{a}(\theta_k)$ and $\boldsymbol{a}(\phi_j)$. The cross-beam power factor of an arbitrary emission sub-pulse which is supposed to radiate from the kth target but reflects from the jth interference can be expressed as

$$p_k(\phi_j) = \boldsymbol{a}^H(\theta_k)\boldsymbol{a}(\phi_j), \quad k = 1, 2, \ldots, K, \ j = 1, 2, \ldots, J \tag{9}$$

Similarly, the cross-beam power factor from ϕ_i to ϕ_j and the vector composed of cross-beam power factor at ϕ_j can be denoted as

$$p_j(\phi_i) = \boldsymbol{a}^H(\phi_j)\boldsymbol{a}(\phi_i), \quad i,j = 1,2,\ldots,J$$
$$\boldsymbol{P}_j(\Phi_J) = \left[\boldsymbol{a}^H(\phi_j)\boldsymbol{a}(\phi_1)\ \ldots \boldsymbol{a}^H(\phi_j)\boldsymbol{a}(\phi_j)\ldots\ \boldsymbol{a}^H(\phi_j)\boldsymbol{a}(\phi_J)\right]^T \tag{10}$$

where $\phi_i, \phi_j \in \Phi_J, i,j \in \{1,2,\ldots,J\}, \boldsymbol{a}^H(\phi_j)\boldsymbol{a}(\phi_j) = M$.

When the location of the target and the interference are known as prior information, the desired spatial shape of the transmitted waveform is composed of peak beam at the target directions and notches at the interference directions.

As mentioned above, in order to reduce the influence of interference on the echo beam of targets and to form notches at the jammer directions, a compensation weight matrix $\boldsymbol{W}$ is introduced, $\boldsymbol{W} = [\boldsymbol{w}_1 \ldots \boldsymbol{w}_k \ldots \boldsymbol{w}_K] \in C^{J*K}$, just like a transmit filter.

There exists a weight matrix that makes the spatial beam formed by the transmit waveform meeting expectation. The synthesized sub-pulse can be easily expressed as

$$\boldsymbol{s}_k^{\dagger}(i) = a(\theta_k)+[a(\phi_1)\ldots a(\phi_j)\ldots a(\phi_J)]\boldsymbol{w_k} \quad i=1,2,\ldots,N_k$$
$$\boldsymbol{w_k} = [w_k(\phi_1)\ldots w_k(\phi_j)\ldots w_k(\phi_J)]^T \quad \phi_j \in \Phi_J \tag{11}$$

Considering the PAPR property of the designed signal and spatial beam pattern matching, an optimized model for $\boldsymbol{S}$ and $\boldsymbol{W}$ can be built as

$$\min_{\boldsymbol{W},\boldsymbol{S}} \sum_{k=1}^{K}\sum_{j=1}^{J}\left|p_k(\theta_j) + \boldsymbol{w}_k^T P_j(\Theta_J)\right|$$
$$\forall k = 1\ldots K,\ \forall j = 1\ldots J$$
$$s.t.\ |s_m(i) - s_m(n)| \le \rho, \quad i,n = 1\ldots K, \forall m = 1,\cdots,M \tag{12}$$

where ρ is a very small positive number, this constraint ensures the transmit energy of different sub-pulses from each element approximately equal. $\boldsymbol{W}$ and $\boldsymbol{S}$ are obtained through optimization.

Generally, $K \ll N, J \ll N$, so the above model can be solved quickly using the CVX toolbox. Then the emission waveform matrix can be obtained by expanding the optimized sub-pulse signal sets as (8).

B. WAVEFORM DESIGN BASED ON ENERGY SPECTRUM DENSITY MATCHING

Considering the practical fact that the ever-growing demand of both high-quality wireless services and accurate remote-sensing capabilities is increasing the amount of required bandwidth, the design of radar signals in a spectrally crowded environment is another topic and challenging problem. Through the above waveform design method, we can get the optimal waveform matrix $\boldsymbol{S}$, which can form a desired beam pattern with peak beam pointing to the directions of target and notches at the interference directions to mitigate spatial interferences. However, in order to suppress interference from other radiator which shares an overlaid frequency band with the MIMO radar, it is necessary to optimize the power spectrum of the transmit waveforms in spectral domain. From (3) and (7), it is obvious that the transmit beam pattern of MIMO radar is only concerned with the correlation of sequences emitting from different elements, then the spectral optimization can be performed through changing the initial phase of the signal sequence. A changing vector Δ is brought in and the new signal matrix is denoted as

$$\begin{aligned}\tilde{\boldsymbol{S}} &= [\boldsymbol{s}(1), \boldsymbol{s}(2), \ldots, \boldsymbol{s}(N)] \odot \Delta\\ &= [\gamma_1 e^{j\varphi_1}\boldsymbol{s}(1), \gamma_2 e^{j\varphi_2}\boldsymbol{s}(2), \ldots, \gamma_N e^{j\varphi_N}\boldsymbol{s}(N)]\\ &= [\tilde{\boldsymbol{s}}(1), \tilde{\boldsymbol{s}}(2), \ldots, \tilde{\boldsymbol{s}}(N)] = [\tilde{\boldsymbol{s}}_1\ \tilde{\boldsymbol{s}}_2 \ldots \tilde{\boldsymbol{s}}_M]^T \in C^{M\times N}\end{aligned} \tag{13}$$

where $\Delta = [\gamma_1 e^{-j\varphi_1}, \gamma_2 e^{-j\varphi_2}, \ldots, \gamma_N e^{-j\varphi_N}]^T, \gamma_n \in R, \varphi_n \in [-\pi, \pi]$.

Then

$$\tilde{\boldsymbol{S}}\tilde{\boldsymbol{S}}^H = \sum_{n=1}^{N} \gamma_n^2 \boldsymbol{s}(n)\boldsymbol{s}^H(n) = N\boldsymbol{R} \tag{14}$$

When $\gamma_1 = \gamma_2 = \ldots = \gamma_N = 1$, Δ is a unit modulus vector, and $\tilde{\boldsymbol{R}} = \boldsymbol{R}$. When $\gamma_1 = \gamma_2 = \ldots = \gamma_N \neq 1, \tilde{\boldsymbol{R}}$ is proportional to $\boldsymbol{R}$. (See the proof in Appendix). It indicates that the change from (1) to (13) has no effect on the MIMO radar spatial beam shape.

In order to ensure the sharing of wireless frequency bands and reduce the interference, the probing energy of MIMO radar in the frequency band shared with other radiators should be the minimized, which is also benefit for diversity reception. According to the definition of the energy spectral density (ESD), the ESD of the m-th array element at the frequency point f can be denoted as

$$P_m(f) = \left|\sum_{n=1}^{N} \tilde{s}_m(n)e^{-j2\pi fn}\right|^2 \tag{15}$$

It can be known from the prior information that there are Q transmitters coexisting in the same frequency band B with the MIMO radar system, and their sub-bands are scattered within the frequency band B. The qth spectral domain interference transmitter works on a sub-band $\Omega_q = \left[f_1^q, f_2^q\right]$, where f_1^q and f_2^q are the lower and upper normalized frequency, respectively. The amount of interfering energy released by M transmitters of MIMO radar system on $\Omega_q = \left[f_1^q, f_2^q\right]$ can be computed as

$$\boldsymbol{E}_I^q = \sum_{m=1}^{M}\int_{f_1^q}^{f_2^q} P_m(f)df = \sum_{m=1}^{M}\tilde{s}_m^H \mathbf{R}_I^q \tilde{s}_m = \boldsymbol{x}^H\tilde{\mathbf{R}}_I^q\boldsymbol{x} \tag{16}$$

where $\mathbf{R}_I^q(i,j) = (f_2^q - f_1^q)e^{j\pi(f_1^k+f_2^k)(i-j)}\sin c(\pi(f_2^k - f_1^k)(i-j)), (i,j) \in \{1,\ldots,N\}^2, \boldsymbol{x} = \mathrm{vec}(\tilde{\boldsymbol{S}}^H)$, and $\tilde{\mathbf{R}}_I^q = \mathbf{R}_I^q \otimes \mathbf{I}_M$.

Let E_I denotes the total amount of interfering energy from Q radiators, which is

$$\boldsymbol{E}_I = \sum_{q=1}^{Q}\omega_q \boldsymbol{x}^H\tilde{\mathbf{R}}_I^q\boldsymbol{x} = \boldsymbol{x}^H(\sum_{q=1}^{Q}\omega_q\tilde{\mathbf{R}}_I^q)\boldsymbol{x} = \boldsymbol{x}^H\tilde{\mathbf{R}}_I\boldsymbol{x} \tag{17}$$

where the non-negative weights $\omega_q, q = 1, \ldots, Q$, represents the relative importance of radiators, is determined based on prior information, and $\sum_{q=1}^{Q} \omega_q = 1$. Therefore, in order to avoid spectrum interference, the power spectrum of the transmitted signal in all the Q sub-band should be minimized, the corresponding optimization model with respect to Δ and ω can be expressed as

$$\min_{\omega,\Delta} (\text{vec}(\tilde{\mathbf{S}}^H))^H (\sum_{q=1}^{Q} \omega_{\boldsymbol{q}} \tilde{\mathbf{R}}_I^q)(\text{vec}(\tilde{\mathbf{S}}^H))$$
$$s.t.\ PAPR(\tilde{s}_m) \leq \rho, \quad i, k = 1 \ldots K\ ,\ \forall m = 1, \cdots, M \tag{18}$$

The spectral interfering energy is considering as an objective function for waveform optimization, which is different from the existing approaches based on constrained non-convex quadratic optimization algorithm. We treat the minimization of E_I as a part of optimization objective in the whole waveform optimization problem to avoid the hard issue of parameter selection. Meanwhile, the constant modulus constraint of Δ is relaxed, which is instead by the PAPR constraint, increasingly decreased the solving complexity with the maintained performance of the solution. The solution method is the same as (12).

IV. SIMULATION RESULTS

In this section, we evaluate the performance of the developed algorithm for joint design of MIMO radar transmit waveform with beam pattern approximation criteria and energy spectral density approximation criteria considering interferences from both spatial domain and spectrum domain in practical environment. We assume the number of transmit antennas is $M = 10$. The code length is $N = 36$ and the total transmit power is $E = 10$. The number of the spatial target is $K = 3$ and the corresponding azimuth set is $\{-30°, 20°, 40°\}$. The number of the spatial jammers is $J = 3$ and the corresponding azimuth set is $\{-50°, 0°, 60°\}$. The associated normalized frequency bands of the spatial jammers are $[f_1^1, f_2^1] = [0.2, 0.3]$, $[f_1^2, f_2^2] = [0.5, 0.6]$ and $[f_1^3, f_2^3] = [0.8, 0.9]$. And the tolerance of the PAPR is $\rho = 2$, while the power limit of the interference band or direction is 10^{-3}.

Meanwhile, the running computation time is analyzed using MATLAB 2021a version, running on a standard PC (with a 11th Gen Intel® Core™ i7-11700 @ 2.50GHz CPU and 32GB RAM).

For comparison with other open literatures, we consider the ideal situation in this subsection, the total energy of the transmitter is uniformly emitted to the K spatial targets and each spectrum interference is suppressed to the same degree. Then, the scale of N_k sub-pulse sets have the same size, $N_k = N/K$, and the weights which are related to the relative importance of the spectrum interference are equal, $\omega_q = 1/Q$. The output beam pattern and PAPR obtained by several existing methods and the proposed method are shown in Fig.1 and Fig.2.

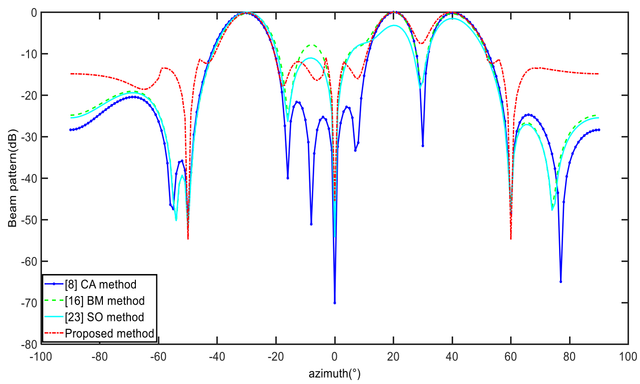

FIGURE 1. Beam pattern after the spatial optimization.

In Fig. 1, these beam patterns basically have the same shape as desired. The total energy of the transmitter is uniformly emitted to the K spatial targets, while there is a nulling at the direction of each spatial interference. From Fig. 1, we can find that there is a little energy imbalance in the results of SO method [23], the amplitude of radiation to the latter two targets is slightly lower than the first one. This phenomenon does not exist in other methods. Meanwhile, the side lobe of the proposed method is lower than other, so the proposed method can yield a good solution for the spatial optimization.

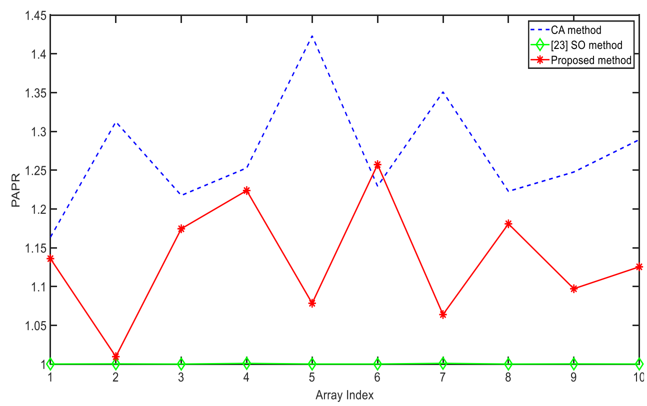

FIGURE 2. PAPR of waveform after the spatial optimization.

AS the BM method [5], [15], [16] does not synthesize waveform. We just calculate the PAPR of waveform synthesized through three other methods during the spatial optimization, the performance of the proposed method is between the method in [23] and the traditional CA method. In Fig.2, the maximum PAPR value of our proposed method is nearly 1.26, which is larger than the result of method in [23] and still within the tolerance.

Also, the computational time of the three method is shown in Table 1, the proposed method spends the shortest time for spatial optimization.

TABLE 1. Time required for the spatial optimization.

	[23] SO method	CA method	Proposed method
Time required (s)	217.519692	2598.2882310	1.560075

Suppose the information of interferences and targets remains unchanged, the code length N and the number of array element M are enlarged, the comparisons of the spatial optimization time is shown in Table 2.

TABLE 2. Time required for the spatial optimization with different M & N.

	M	N	[23] SO method	CA method	Proposed method
Time required (s)	10	24	64.74	1034.573	0.972
	10	36	220.342	2598.288	1.560
	15	36	523.330	10392.954	1.862

Simultaneously, we simulate the energy spectral density of the waveform after spatial optimization in Fig. 3. Different from the results of the other two methods, the ESD of the propose method is periodic, which is determined by the proposed waveform synthesis method and will not affect the final design result. As the proposed method have divided subpulse signals in the fast time into K group before spatial optimization. The emission waveform obtained through spatial optimization is a combination of intercepts of several periodic signals, so there are discrete periodic spectrum components in the power spectrum of the optimized waveform. The distribution of the energy spectrum is consistent with the structure of the waveform.

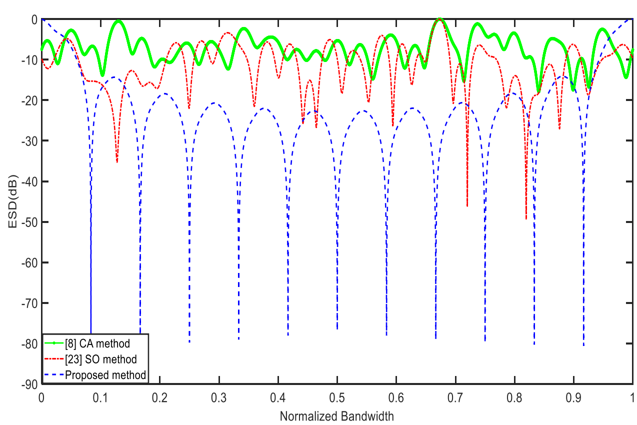

FIGURE 3. ESD of waveform after the spatial optimization.

Next, we check the performance of the proposed method in spectral domain, and compare with the method proposed in [23], which are the closest method to each other. The output beam pattern formed by the waveform obtained by spectral

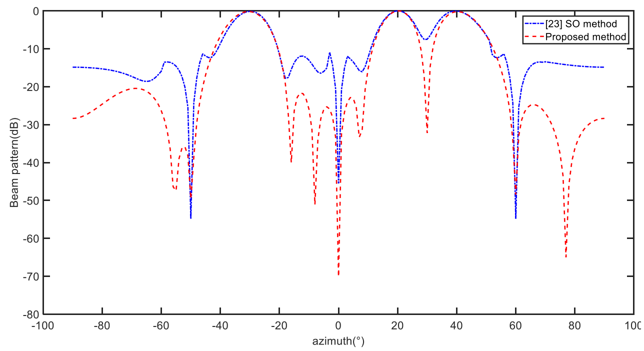

FIGURE 4. Beam pattern after the spatial-spectral optimization.

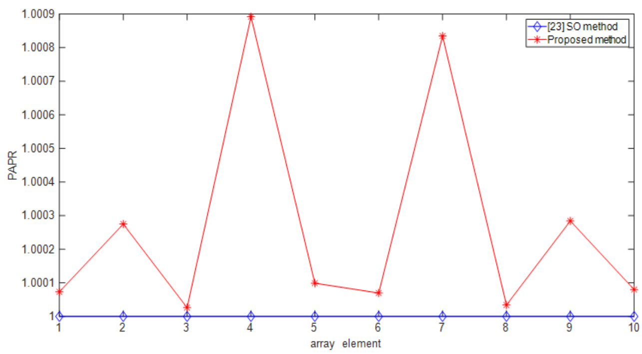

FIGURE 5. PAPR of waveform after the spatial-spectral optimization.

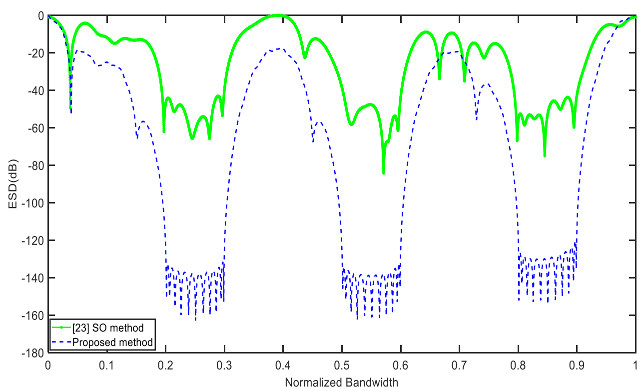

FIGURE 6. ESD of waveform after the spatial-spectral optimization.

optimization is shown in Fig. 4, which is almost the same as Fig. 1. The spectrum optimization of the emission waveform does not change the correlation of the array element waveform, and the corresponding beam pattern of emission waveform is not changed. It verifies that the spatial-spectral optimization can be carried out sequentially.

The PAPR and ESD of the waveform obtained after spectral optimization are shown in Fig.5 and Fig.6. From Fig. 5, we can see that the maximum PAPR value of our proposed method is nearly 1.009, which is better than the value before the spectrum optimization. Compared with Fig.2, PAPR value becomes smaller. It indicates that using the PAPR constraint again improves the PAPR of the final designed waveform.

The ESD of the optimized waveform shown in Fig.6 has three nulls in the three interference sub-bands as expected, and the proposed method has a nulling depth of up to -140dB. As the modulus of the changing vector Δ is small, the shape of ESD has not changed too much. As the CA algorithm does not perform spectral domain optimization, the comparison is only between two algorithms.

V. CONCLUSION

In this paper, we have addressed the problem of spatial-spectral joint anti-jamming design of centralized MIMO radar transmit waveform in a multi-target and multi-interference scenario. The proposed method is to execute the spatial-spectral domain design sequentially. Different with the existing methods, we divide the emission signal into several sub-pulse sets and combine the cross-beam energy and the weighted of interfering energy from the spatial interference as the optimization objective under a PAPR constraint instead of the constant modulus, such that avoid solving a non-convex problem. The beam pattern obtained after spatial optimization meets the expectation. And the computational burden of our proposed algorithm is significantly decreased. Then a similar model is built and solved for further spectral optimization. Besides, we have compared the performance of the proposed sequential algorithm with another joint optimization method in the spatial optimization and the spectral optimization, sequentially. Our devised algorithm not only outperforms the existing methods with respect of beam pattern and ESD but also enjoys a high efficiency.

APPENDIX

PROOF THE RELATION OF $\tilde{R}$ AND R

Denote the original signal matrix as $\boldsymbol{S}$, and

$$\boldsymbol{S} = [\boldsymbol{s}(1), \boldsymbol{s}(1), \ldots, \boldsymbol{s}(N)] = [s_1 s_2 \ldots s_M]^T \in C^{M\times N} \quad (19)$$

The covariance matrix often has an approximately equal relationship with the statistical average of the signal sequence covariance matrix. Usually expressed as

$$\boldsymbol{R} = \frac{1}{N}\sum_{n=1}^{N} s(n)s^H(n) = \frac{1}{N}\boldsymbol{S}\boldsymbol{S}^H \quad (20)$$

Denote the element in the m th row and n th column of the matrix $\boldsymbol{S}$ as $\boldsymbol{s_{mn}}$, then

$$\boldsymbol{S}\boldsymbol{S}^H = \begin{bmatrix} s_{11} & s_{12} & \ldots & s_{1N} \\ s_{21} & s_{22} & \ldots & s_{2N} \\ \ldots & \ldots & \ldots & \ldots \\ s_{M1} & s_{2N} & \ldots & s_{MN} \end{bmatrix} \times \begin{bmatrix} s_{11}^* & s_{21}^* & \ldots & s_{M1}^* \\ s_{12}^* & s_{22}^* & \ldots & s_{M2} \\ \ldots & \ldots & \ldots & \ldots \\ s_{1N}^* & s_{2N}^* & \ldots & s_{MN}^* \end{bmatrix} = \begin{bmatrix} s_1 s_1^* & s_1 s_2^* & \ldots & s_1 s_M^* \\ s_2 s_1^* & s_2 s_2^* & \ldots & s_2 s_M^* \\ \ldots & \ldots & \ldots & \ldots \\ s_M s_1^* & s_M s_2^* & \ldots & s_M s_M^* \end{bmatrix} = N\boldsymbol{R} \quad (21)$$

Define the phase changing vector Δ is

$$\Delta = [\gamma_1 e^{-j\varphi_1}, \gamma_2 e^{-j\varphi_2}, \ldots, \gamma_N e^{-j\varphi_N}]^T, \quad \gamma_n \in R, \varphi_n \in [-\pi, \pi] \quad (22)$$

The new signal matrix is

$$\begin{aligned}\tilde{\boldsymbol{S}} &= [\boldsymbol{s}(1), \boldsymbol{s}(2), \ldots, \boldsymbol{s}(N)] \odot \Delta \\ &= [\gamma_1 e^{-j\varphi_1}\boldsymbol{s}(1), \gamma_2 e^{-j\varphi_2}\boldsymbol{s}(2), \ldots, \gamma_N e^{-j\varphi_N}\boldsymbol{s}(N)] \quad (23)\end{aligned}$$

Then

$$\tilde{\boldsymbol{S}} = \begin{bmatrix} \gamma_1 e^{-j\varphi_1} s_{11} & \gamma_2 e^{-j\varphi_2} s_{12} & \ldots & \gamma_N e^{-j\varphi_N} s_{1N} \\ \gamma_1 e^{-j\varphi_1} s_{21} & \gamma_2 e^{-j\varphi_2} s_{22} & \ldots & \gamma_N e^{-j\varphi_N} s_{2N} \\ \ldots & \ldots & \ldots & \ldots \\ \gamma_1 e^{-j\varphi_1} s_{M1} & \gamma_2 e^{-j\varphi_2} s_{2N} & \ldots & \gamma_N e^{-j\varphi_N} s_{MN} \end{bmatrix}.$$

And

$$\tilde{\boldsymbol{S}}\tilde{\boldsymbol{S}}^H = \sum_{n=1}^{N} \gamma_n^2 \boldsymbol{s}(n)\boldsymbol{s}^H(n) = \sum_{n=1}^{N} \gamma_n^2 \boldsymbol{R}_n = N\tilde{\boldsymbol{R}} \quad (24)$$

where $\boldsymbol{R}_n = \boldsymbol{s}(n)\boldsymbol{s}^H(n) \in C^{M*M}$ is the covariance matrix of the nth signal sequence.

It yields

$$\begin{aligned}\tilde{\boldsymbol{S}}\tilde{\boldsymbol{S}}^H &= \begin{bmatrix} \gamma_1 e^{-j\varphi_1} s_{11} & \ldots & \gamma_N e^{-j\varphi_N} s_{1N} \\ \gamma_1 e^{-j\varphi_1} s_{21} & \ldots & \gamma_N e^{-j\varphi_N} s_{2N} \\ \ldots & \ldots & \ldots \\ \gamma_1 e^{-j\varphi_1} s_{M1} & \ldots & \gamma_N e^{-j\varphi_N} s_{MN} \end{bmatrix} * \begin{bmatrix} \gamma_1 e^{j\varphi_1} s_{11}^* & \ldots & \gamma_1 e^{j\varphi_N} s_{M1}^* \\ \gamma_2 e^{j\varphi_2} s_{12}^* & \ldots & \gamma_2 e^{j\varphi_N} s_{M2} \\ \ldots & \ldots & \ldots \\ \gamma_N e^{j\varphi_N} s_{1N}^* & \ldots & \gamma_N e^{j\varphi_N} s_{MN}^* \end{bmatrix} \\ &= \begin{bmatrix} \sum_{n=1}^{N} \gamma_n^2 s_{1n} s_{1n}^* & \sum_{n=1}^{N} \gamma_n^2 s_{1n} s_{2n}^* & \ldots & \sum_{n=1}^{N} \gamma_n^2 s_{1n} s_{Mn}^* \\ \sum_{n=1}^{N} \gamma_n^2 s_{2n} s_{1n}^* & \sum_{n=1}^{N} \gamma_n^2 s_{2n} s_{2n}^* & \ldots & \sum_{n=1}^{N} \gamma_n^2 s_{2n} s_{Mn}^* \\ \ldots & \ldots & \ldots & \ldots \\ \sum_{n=1}^{N} \gamma_n^2 s_{Mn} s_{1n}^* & \sum_{n=1}^{N} \gamma_n^2 s_{Mn} s_{2n}^* & \ldots & \sum_{n=1}^{N} \gamma_n^2 s_{Mn} s_{Mn}^* \end{bmatrix} \\ &= \begin{bmatrix} \gamma_1^2 \\ \gamma_2^2 \\ \ldots \\ \gamma_N^2 \end{bmatrix}^T \odot \begin{bmatrix} s_1^T \odot s_1^H & s_1^T \odot s_2^H & \ldots & s_1^T \odot s_M^H \\ s_2^T \odot s_1^H & s_2^T \odot s_2^H & \ldots & s_2^T \odot s_1^H \\ \ldots & \ldots & \ldots & \ldots \\ s_M^T \odot s_1^H & s_M^T \odot s_2^H & \ldots & s_M^T \odot s_M^H \end{bmatrix} \\ &= kron(\upsilon, \Upsilon) \quad (25)\end{aligned}$$

where $kron()$ stands for Kronecker product, and $\upsilon = [\gamma_1^2\ \gamma_2^2\ \ldots\ \gamma_N^2]$, $\Upsilon_{ij} = [s_i^T \odot s_j^H]$, $\{i, j\} \in 1 \ldots M$.

If $\gamma_1 = \gamma_2 = \ldots = \gamma_N = 1$, compared (25) with(21), we have that

$$N\tilde{\boldsymbol{R}} = \begin{bmatrix} 1 \\ 1 \\ \ldots \\ 1 \end{bmatrix}^T \odot \begin{bmatrix} s_1^T \odot s_1^H & \ldots & s_1^T \odot s_M^H \\ s_2^T \odot s_1^H & \ldots & s_2^T \odot s_M^H \\ \ldots & \ldots & \ldots \\ s_M^T \odot s_1^H & \ldots & s_M^T \odot s_M^H \end{bmatrix}$$

$$= \begin{bmatrix} s_1 s_1^* & \dots & s_1 s_M^* \\ s_2 s_1^* & \dots & s_2 s_M^* \\ \dots & \dots & \dots \\ s_M s_1^* & \dots & s_M s_M^* \end{bmatrix} = N\boldsymbol{R} \tag{26}$$

If $\gamma_1 = \gamma_2 = \ldots = \gamma_N \neq 1$, $\tilde{\boldsymbol{R}}$ is proportional to $\boldsymbol{R}$.

Therefore, the proof of the relation of $\tilde{\boldsymbol{R}}$ and $\boldsymbol{R}$ is completed.

REFERENCES

[1] P. Wang and H. Li, "Target detection with imperfect waveform separation in distributed MIMO radar," *IEEE Trans. Signal Process.*, vol. 68, pp. 793–807, 2020.

[2] N. Aboutorab, W. Hardjawana, and B. Vucetic, "Interference cancellation in multi-user MIMO relay networks using beamforming and precoding," in *Proc. IEEE Wireless Commun. Netw. Conf.*, Sydney, NSW, Australia, Apr. 2010, pp. 18–21.

[3] U. K. Majumder, M. R. Bell, and M. Rangaswamy, "A novel approach for designing diversity radar waveforms that are orthogonal on both transmit and receive," in *Proc. IEEE Radar Conf. (RadarCon)*, Ottawa, ON, Canada, Apr. 2013, pp. 1–6.

[4] S. Ahmed and M.-S. Alouini, "MIMO radar transmit beampattern design without synthesising the covariance matrix," *IEEE Trans. Signal Process.*, vol. 62, no. 9, pp. 2278–2289, May 2014.

[5] N. Pandey and L.-P. Roy, "Convex optimisation based transmit beampattern synthesis for MIMO radar," *Electron. Lett.*, vol. 52, no. 9, pp. 761–763, Feb. 2016.

[6] H.-S. Xu, R.-S. Blum, J. Wang, and J. Yuan, "Colocated MIMO radar waveform design for transmit beampattern formation," *IEEE Trans. Aerosp. Electron. Syst.*, vol. 51, no. 2, pp. 1558–1568, May 2015.

[7] T. Ni, S. Liu, Z. Mao, and Y. Huang, "Range-dependent beamforming using space-frequency virtual difference coarray," in *Proc. IEEE Radar Conf.*, Atlanta, GA, USA, May 2021, pp. 1–5.

[8] P. Stoica, J. Li, and X. Zhu, "Waveform synthesis for diversity-based transmit beampattern design," *IEEE Trans. Signal Process.*, vol. 56, no. 6, pp. 2593–2598, Jun. 2008.

[9] W. Fan, J. Liang, and J. Li, "Constant modulus MIMO radar waveform design with minimum peak sidelobe transmit beampattern," *IEEE Trans. Signal Process.*, vol. 66, no. 16, pp. 4207–4222, Aug. 2018.

[10] Z. Cheng, Z. He, B. Liao, and M. Fang, "MIMO radar waveform design with PAPR and similarity constraints," *IEEE Trans. Signal Process.*, vol. 64, no. 4, pp. 968–981, Feb. 2017.

[11] G. Pengcheng, L. Zheng, and W. Jingjing, "Radar group target recognition based on HRRPs and weighted mean shift clustering," *J. Syst. Eng. Electron.*, vol. 31, no. 6, pp. 1152–1159, Dec. 2020.

[12] Y. Huiming and X. Fuxin, "A remote sensing image target recognition method based on improved mask-RCNN model," in *Proc. IEEE 2nd Int. Conf. Big Data, Artif. Intell. Internet Things Eng. (ICBAIE)*, Mar. 2021, pp. 436–439.

[13] M. P. Masarik and N. S. Subotic, "Cramèr-Rao lower bounds for radar parameter estimation in noise plus structured interference," in *Proc. IEEE Radar Conf. (RadarConf)*, May 2016, pp. 1–4.

[14] L. H. Nguyen and T. D. Tran, "Estimation and extraction of radio-frequency interference from ultra-wideband radar signals," in *Proc. IEEE Int. Geosci. Remote Sens. Symp. (IGARSS)*, Jul. 2015, pp. 2848–2851.

[15] X. Liu, T. Huang, N. Shlezinger, Y. Liu, J. Zhou, and Y. C. Eldar, "Joint transmit beamforming for multiuser MIMO communications and MIMO radar," *IEEE Trans. Signal Process.*, vol. 68, pp. 3929–3944, 2020.

[16] Y. Liu, Z. Liu, R. Xie, Q. Liu, and X. Wu, "Transmit beampattern synthesis and performance analysis for collocated MIMO radar," in *Proc. Int. Conf. Radar*, Sep. 2013, pp. 188–193.

[17] B. Tang, J. Li, and J. Liang, "Alternating direction method of multipliers for radar waveform design in spectrally crowded environments," *Signal Process.*, vol. 142, pp. 398–402, Jan. 2018.

[18] A. Aubry, A. De Maio, Y. Huang, M. Piezzo, and A. Farina, "A new radar waveform design algorithm with improved feasibility for spectral coexistence," *IEEE Trans. Aerosp. Electron. Syst.*, vol. 51, no. 2, pp. 1029–1038, Apr. 2015.

[19] A. Aubry, A. De Maio, M. Piezzo, and A. Farina, "Radar waveform design in a spectrally crowded environment via nonconvex quadratic optimization," *IEEE Trans. Aerosp. Electron. Syst.*, vol. 50, no. 2, pp. 1138–1152, Apr. 2014.

[20] Y. Feng, T. Shan, S. Liu, and R. Tao, "Interference suppression using joint spatio-temporal domain filtering in passive radar," in *Proc. IEEE Radar Conf. (RadarCon)*, Arlington, VA, USA, May 2015, pp. 1156–1160.

[21] O. Aldayel, V. Monga, and M. Rangaswamy, "Successive QCQP refinement for MIMO radar waveform design under practical constraints," *IEEE Trans. Signal Process.*, vol. 64, no. 14, pp. 3760–3774, Jul. 2016.

[22] C.-H. Chu, Y.-J. Chen, Q. Zhang, and Y. Luo, "MIMO radar waveform joint optimization design in time and frequency domain," in *Proc. IEEE 11th Sensor Array Multichannel Signal Process. Workshop (SAM)*, Jun. 2020, pp. 1–5.

[23] Q.-L. Zhai, Y.-X. Wang, and W. Li, "MIMO radar transmit beampattern design with PAR constraint in a spectrally crowded environment," in *Proc. Int. Conf. Comput. Netw. Commun. Technol. (CNCT)*, Jan. 2017, pp. 16–18.

[24] P. M. McCormick, S. D. Blunt, and J. G. Metcalf, "Joint spectrum/beampattern design of wideband FM MIMO radar emissions," in *Proc. IEEE Radar Conf. (RadarConf)*, May 2016, pp. 1–6.

CHUN-HUA CHU was born in Hubei, China, in 1981. She received the M.S. degree in control theory and control engineering from the School of Automation, Wuhan University of Technology, Wuhan, China, in 2006. She is currently pursuing the Ph.D. degree in electrical engineering with the Institute of Information and Navigation, AFEU. She is currently a Lecturer with the School of Mechanical and Electrical Engineering, Hainan University. Her current research interests include signal processing and radar waveform optimization design.

QUN ZHANG received the M.S. degree in mathematics from Shaanxi Normal University, Xi'an, China, in 1988, and the Ph.D. degree in electrical engineering from Xidian University, Xi'an, in 2001. He was a Research Engineer and a Research Fellow with the Department of Electrical and Computer Engineering, National University of Singapore, Singapore, from 2001 to 2003 and from 2005 to 2006, respectively. He has published over 200 papers on journals and conferences. His research interests include signal processing, clutter suppression, and its application in SAR and ISAR.

YI-JUN CHEN was born in Shaanxi, China, in 1989. She received the M.S. and Ph.D. degrees in electrical engineering from the Institute of Information and Navigation, Air Force Engineering University (AFEU), Xi'an, China, in 2013 and 2017, respectively. She is currently working with the College of Information Engineering, Engineering University of PAP, Xi'an. She has published one book and over 20 papers on journals and conferences. Her current research interests include signal processing and cognitive radar.